



SLIP SOURCE MODEL OF THE 1995 NEFTEGORSK EARTHQUAKE (NORTH SAKHALIN) FROM GEODETIC DATA

A.S. Prytkov  , N.F. Vasilenko 

Institute of Marine Geology and Geophysics, Far Eastern Branch of the Russian Academy of Sciences, 1B Nauki St, Yuzhno-Sakhalinsk 693022, Russia

ABSTRACT. The May 27, 1995 $M_w=7.0$ Neftegorsk earthquake occurred in the north of Sakhalin Island, rupturing the Upper Piltun fault, a secondary feature of the main Hokkaido-Sakhalin regional fault zone. The fault geometry, coseismic slip model, and Coulomb stress changes in the earthquake focal area were calculated based on a finite fault modeling. We used near-field coseismic offsets at 24 points obtained by comparison between predating triangulation and GPS observations, which were collected before and after the earthquake. Our slip distribution model shows two major slip patches. Larger slip asperity (amplitude up to 6.36 m) was characterized by right-lateral strike-slip movements, which correspond to focal mechanism of the earthquake, whereas the northern segment has reverse fault mechanism with maximum slip of 2.64 m. The fault length and width, average slip and stress drop values are estimated at 78 km, 28 km, 1.91 m and 11.3 MPa, respectively. The estimated release moment is approximately 7.49×10^{19} N·m equal to $M_w=7.2$, which is larger than that reported by the USGS and GCMT but consistent with the values reported by other researchers. The coseismic Coulomb stress changes enhanced the stress by more than 10 MPa on the southern segment of the Gyrgylaninsky fault and middle section of the Hokkaido-Sakhalin fault. Seismic risks on the nearest faults cannot be ignored in the future despite the fact that the earthquake with a magnitude of 5.8 occurred in 2010 near the Gyrgylaninsky fault. The recent GPS rates in the surroundings of the Neftegorsk surface rupture mean that the recurrence interval for similar earthquakes may be more than a thousand years.

KEYWORDS: Neftegorsk earthquake; coseismic displacements; slip model; inversion

FUNDING: The research was carried out within the state assignment of IMGG FEB RAS, with the support of the Ministry of Science and Higher Education of the Russian Federation (theme 121022000085-9).



RESEARCH ARTICLE

Correspondence: Alexander S. Prytkov, a.prytkov@imgg.ru

Received: February 10, 2023

Revised: April 3, 2023

Accepted: April 11, 2023

FOR CITATION: Prytkov A.S., Vasilenko N.F., 2023. Slip Source Model of the 1995 Neftegorsk Earthquake (North Sakhalin) from Geodetic Data. *Geodynamics & Tectonophysics* 14 (4), 0712. doi:10.5800/GT-2023-14-4-0712

МОДЕЛЬ ОЧАГА НЕФТЕГОРСКОГО ЗЕМЛЕТРЯСЕНИЯ 1995 ГОДА (СЕВЕРНЫЙ САХАЛИН) НА ОСНОВЕ ГЕОДЕЗИЧЕСКИХ ДАННЫХ

А.С. Прытков, Н.Ф. Василенко

Институт морской геологии и геофизики ДВО РАН, 693022, Южно-Сахалинск, ул. Науки, 1Б, Россия

АННОТАЦИЯ. 27 мая 1995 года на севере острова Сахалин произошло землетрясение $M_w=7.0$, в результате которого вскрылся Верхнепильтунский сейсморазрыв – вторичный сегмент главной Хоккайдо-Сахалинской разломной зоны региона. Геометрия сейсморазрыва, косейсмические смещения и изменение кулоновских напряжений в очаговой области рассчитаны на основе модели конечного источника. Для моделирования использовались косейсмические смещения 24 пунктов, которые получены путем сравнения данных триангуляции и GPS-наблюдений до и после землетрясения. Моделированием установлены два основных участка разрывных нарушений с различным распределением смещений. Большой участок (с амплитудой 6.36 м) характеризуется правосторонними сдвиговыми смещениями, направление которых соответствует механизму очага землетрясения, в то время как северный сегмент сейсморазрыва имел противоположную подвижку с локальной амплитудой смещения 2.64 м. Длина и ширина разлома, средние значения смещений и сброшенных напряжений составили 78 км, 28 км, 1.91 м и 11.3 МПа соответственно. Расчетный сейсмический момент 7.49×10^{19} Н·м соответствует магнитуде $M_w=7.2$ и несколько больше оценок USGS и GCMT, однако согласуется с данными других исследований. Косейсмическое приращение кулоновского напряжения более чем на 10 МПа выявлено в южном сегменте Гырғыланьинского и центральной части Хоккайдо-Сахалинского разлома. Несмотря на то, что на Гырғыланьинском разломе в 2010 г. произошло землетрясение магнитудой 5.8, сейсмическую опасность в районе исследований нельзя игнорировать в будущем. Величины современных скоростей GPS-пунктов в окрестности Нефтегорского сейсморазрыва свидетельствуют о том, что период повторяемости подобных землетрясений может составлять более тысячи лет.

КЛЮЧЕВЫЕ СЛОВА: Нефтегорское землетрясение; косейсмические смещения; модель конечного источника; инверсия

ФИНАНСИРОВАНИЕ: Исследование выполнено в рамках государственного задания ИМГГ ДВО РАН при поддержке Минобрнауки РФ (тема № 121022000085-9).

1. INTRODUCTION

On May 27, 1995, a large earthquake with the moment magnitude of $M_w=7.0$ occurred in the north of Sakhalin Island (Russia). The epicenter was located at 52.629°N and 142.827°E , about 40 km southwest of the Neftegorsk city, with the hypocenter depth of 11 km [USGS..., 2022] (Fig. 1). The earthquake caused severe damages in the Neftegorsk city. Many houses were destroyed, and the number of earthquake victims exceeded 2000.

This earthquake was the largest seismic event for the instrumental period of seismological observations on Sakhalin Island. Since 1905, earthquakes in this area had a magnitude no more than 5.6. The mainshock was located at the junction of the Eurasian and North American plates which stretches along Sakhalin Island from north to south. In this area, the Eurasian plate moves eastward relative to stable North America at a rate of 6 mm/yr [DeMets et al., 2010]. The earthquake focal mechanism estimated by the Global Centroid Moment Tensor Database [Global CMT..., 2022] has a nodal plane with a south strike of 196° and a dip angle of 82° , and another nodal plane with a northwest strike of 287° and a dip angle of 79° . The focal mechanism of the event indicates a steeply dipping right-lateral fault if the N-S nodal plane is considered as working plane.

Coseismic surface ruptures are associated with the Upper Piltun fault, a secondary feature joining the Hokkaido-Sakhalin fault, which is one of the main tectonic elements of the region. The Upper Piltun fault has been moving right-laterally during the late Quaternary time at the average rate of 3–5 mm/yr. Trenching of the fault as well as radiocarbon dating of the faulted strata and landscape features showed that fault-related strong earthquakes took place with an interval of several hundred to one or two thousand years interval [Kozhurin, 2004]. According to the field investigation, the length of the surface rupture is approximately 35 km [Shimamoto et al., 1996]. [Rogozhin, 1995] described the branch rupture to the north of the Neftegorsk city and adopted that the rupture reaches 46 km in length. The maximum right-lateral displacement along the fault reached 8.1 m in its northern part, at 52.88°N , and the maximum vertical offset was 1.8 m. The average lateral displacement on the Earth's surface was 3.8 m [Shimamoto et al., 1996].

The largest aftershock $M_w=5.6$ occurred half a year after the mainshock. Most of the aftershocks were located at a depth less than 15 km. The length of the aftershock area was approximately 60 km [Arefiev et al., 2000; Katsumata et al., 2004], which is significantly longer than the lengths

of the surface rupture. The western part of the aftershocks area included more epicenters than the eastern part of the surface rupture. It indicates that the main nodal plane is dipping to the west.

Several researchers studied the slip distribution during the earthquake by inversion of coseismic crustal deformations. In work [Takahashi et al., 1996] determined the parameters of the simple rectangular fault plane by comparison between predated triangulation and position of

12 GPS observation points. The length of rectangular dislocation fault model was 35 km, width was 15 km. The angles of strike, dip and slip were 17°, 78° and 165°, respectively. Slip rupture was estimated at 5.5 m. In [Tobita et al., 1998] estimated optimal coseismic slip parameter for 12 subfaults using SAR interferograms. The inversion showed that the total rupture area extends to 48.1 km, and slip varies from 0.2 to 7.1 m from the south to the north of the fault plane. They also suggested that a hidden fault may

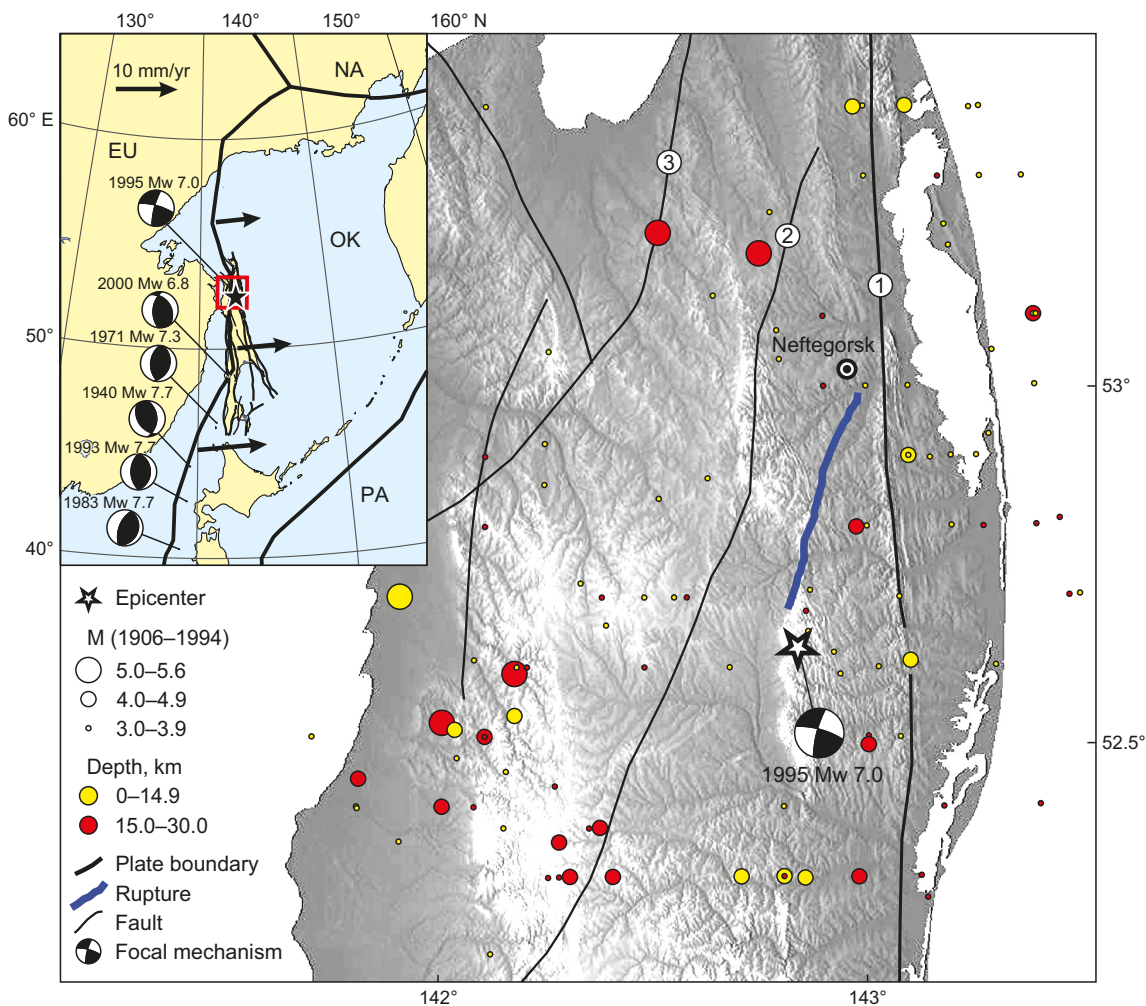


Fig. 1. The tectonic setting of the 1995 Neftegorsk earthquake.

Black thin lines are active faults from [Kharakhinov, 2010]: 1 – Hokkaido–Sakhalin, 2 – Gyrgylaninsky, 3 – Western Baikal. Blue line is the Neftegorsk surface rupture. Red and yellow circles represent earthquakes $M \geq 3$ in 1906–1994 from the Geophysical Survey of the Russian Academy of Sciences [GS RAS..., 2022]. Insert: the rectangle shows the study area. The mainshock epicenter (asterisk) and its mechanism are from [USGS..., 2022]; the focal mechanisms (lower hemisphere) of strong earthquakes along the boundary (black bold line) of the Okhotsk plate (OK) and the Eurasian plate (EU) are from [Katsumata et al., 2004]. PA – Pacific plate; NA – North American plate. Arrows indicate the motion of the Eurasian plate relative to the stable North America plate by based on MORVEL model [DeMets et al., 2010].

Рис. 1. Тектоническое положение Нефтегорского землетрясения 1995 г.

Черными линиями показаны активные разломы [Kharakhinov, 2010]: 1 – Хоккайдо–Сахалинский, 2 – Гыргыланьинский, 3 – Западно-Байкальский. Синяя линия – сейсморазрыв Нефтегорского землетрясения. Эпицентры землетрясений $M \geq 3$ с 1906 по 1994 г. приведены по данным ФИЦ «Единая геофизическая служба РАН» [GS RAS..., 2022]. На врезке: прямоугольником показан район исследований. Эпицентр главного толчка (звездочка) и механизм очага приведены по данным [USGS..., 2022], механизмы очагов сильных землетрясений (в проекции нижней полусферы) вдоль границы Охотской (OK) и Евразийской плиты (EU) (черная жирная линия) – по [Katsumata et al., 2004]. PA – Тихоокеанская плита; NA – Североамериканская плита. Стрелками обозначено направление и скорость движения Евразийской плиты относительно Североамериканской согласно модели MORVEL [DeMets et al., 2010].

be existing in the northern end of the seismic fault, which moved right-laterally after the mainshock. This source model is finer than the model derived from GPS observations [Takahashi et al., 1996] because SAR interferograms yielded much more information. In [Polets, Zlobin, 2017] estimated the rupture process and the slip distribution by teleseismic waveform inversion. They identified the fault plane which is 80 km long and 30 km wide. Inversion results indicated that a seismic rupture was initiated at the southern part of the source area and propagated to NNE. The duration of the rupture process was ~27 s and had two main peaks with the maximum slip values to 6.62 m. The seismic moment totaled 7.7×10^{19} N·m, which is equal to $M_w=7.19$.

In this study, the rupture of the Neftegorsk earthquake is estimated by the finite fault source inversion method. Finite fault rupture models provide a valuable resource to investigate and better understand earthquake source processes, which is more reliable for regional seismic hazard analysis. A slip model is calculated from the near-field coseismic displacements. Geodetic data provide better constraints on the rupture area, maximum slip and surface rupture as compared with the inversion results from teleseismic body waves. Furthermore, the Coulomb stress changes were also calculated using the model coseismic

slip distribution in order to better understand earthquake source process.

2. DATA AND METHODS

Crustal deformations caused by the Neftegorsk earthquake were detected by the GPS network [Takahashi et al., 1995]. In this study, we used the near-field static coseismic displacements obtained by comparison between the predating triangulation data and positions of 24 GPS observation points collected before and after the earthquake [Vasilenko et al., 2015]. Making amendments between triangulation data and GPS observations allowed us to achieve average errors in the horizontal and vertical components of displacements up to 15 cm and 10 cm, respectively. Fig. 2 shows horizontal and vertical components of coseismic displacements. The distribution of the geodetic points is not uniform, but they cover the immediate surroundings bounding the eastern and western sides of surface rupture. The maximum displacements of geodetic points were found to be 2.15 m in horizontal and 1.02 m in vertical direction. In the northwestern research area, coseismic displacements show almost north offsets and uplift of the earth surface. In the southeast, coseismic displacements show offsets in the southwest direction, the vertical displacements have small values. Although

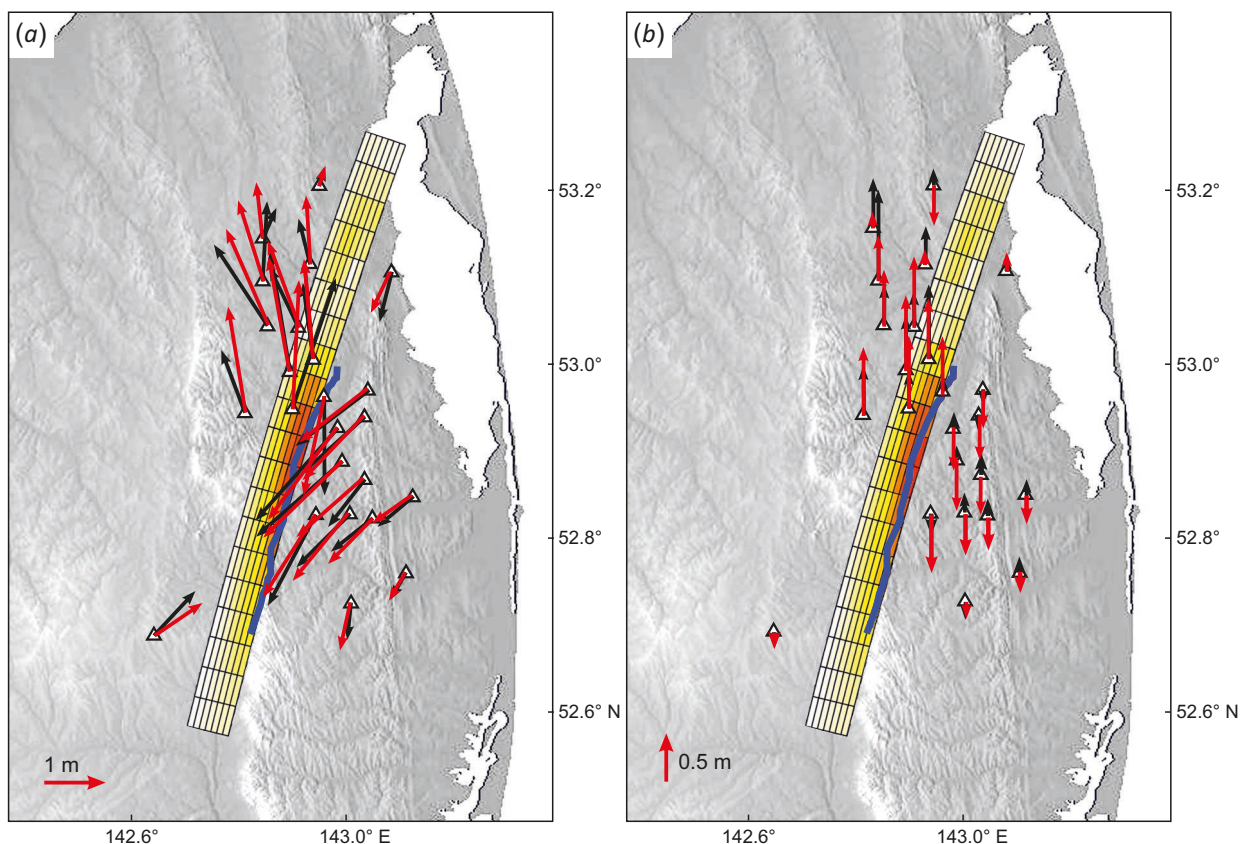


Fig. 2. Observed (black) and model (red) coseismic horizontal (a) and vertical (b) displacements of 24 GPS points used in the study. There is shown the slip model of the Neftegorsk earthquake (yellow to red). Blue line shows the surface rupture.

Рис. 2. Измеренные (черные) и модельные (красные) косейсмические горизонтальные (a) и вертикальные (b) смещения 24 GPS-пунктов, использованных в исследовании. Показана модель Нефтегорского землетрясения (цвет от желтого к красному). Синяя линия – поверхностный сейсморазрыв.

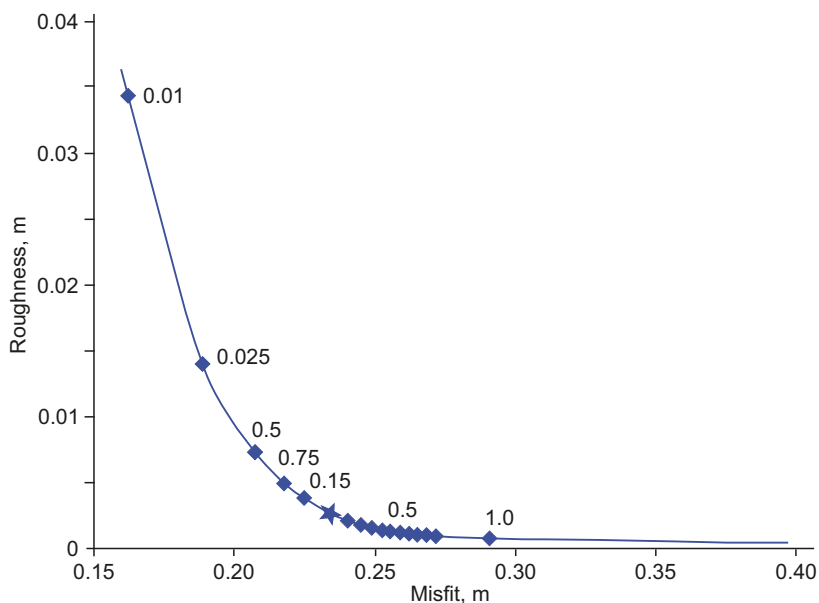


Fig. 3. Trade-off curve between the data misfit and slip roughness of model. The optimal smoothing factor is marked by asterisk.
Рис. 3. Кривая согласования модельных невязок. Оптимальный коэффициент сглаживания отмечен звездочкой.

the postseismic effects following the mainshock may be included in the estimated coseismic displacements, their values should be small in comparison with the coseismic components. All three components of the revealed coseismic displacements were used to model the rupture source of the earthquake.

Based on the aftershock distribution [Katsumata et al., 2004] and field geological investigations [Shimamoto et al., 1995], at first we outlined the fault trace striking north-south in the range from 200° to 196°. We determined the source parameters using analytical solutions of a rectangular dislocation in a homogeneous elastic half-space [Okada, 1985] and assuming Poisson ratio of 0.25. In this study, the optimization procedure was realized using the steepest descent method (SDM) incorporated layered crust structure and curved fault geometry [Wang et al., 2013]. We evaluated the slip model according to data-fitting quality of the residuals between observed and modeled displacements by root mean square errors (RMSE). A priori constraint of the model included upper limit 10 m of a slip. The constraints are needed to obtain a smooth slip model, which can be realized through a factor minimizing data misfit. The optimal smoothing model was obtained through adjusting the normalized smoothing factor, which was determined by using a trade-off value between model roughness and data misfit. Higher roughness corresponding to lower smoothing factor provides lower misfit, while lower roughness, corresponding to high smoothness, provides higher misfit [Segall, Harris, 1987]. We chose 0.15 as the best slip distribution smoothing factor at the inflection point of the trade-off curve (Fig. 3). During coseismic slip modeling, we tested different fault dip angles and the fault length and width by many trial computations. The fault length and width were set to 78 km and 28 km, respectively. The fault plane was divided into 20×7 subfaults of

3.9×4 km along the strike and dip directions. Optimal dip angle was assumed to be 79°.

3. RESULTS

The obtained solution is characterized by high correlation coefficient 0.979, indicating excellent consistency between the observed and model data. Overall, the comparisons between the observed and modeled displacements demonstrate small misfits (see Fig. 2). According to residual distributions, the solution for horizontal displacements is better than that for vertical. The directions of the modeled horizontal displacements are consistent with the observed values. The average square residual between the measured and modeled values for northern and eastern components is 0.03 and 0.04, respectively. The average square residual between the observed and modeled vertical displacements is 0.13. Some local misfits eastward from the rupture may be related to heterogeneity, unaccounted for by our elastic half-space model, as well as postseismic effects, which may exist in the observed coseismic displacements.

The slip model of the Neftegorsk earthquake inverted from the geodetic data is shown in Fig. 4. The slip shows mainly right-lateral strike-slip motions. The slip model indicates that the earthquake rupture reached the earth surface. The model dipping plane suggests two asperities. The first patch is concentrated at a shallow depth and extends ~40 km along the strike. This larger slip asperity has maximum slip of 6.36 m near the surface (at 52.87 °N, 142.91 °E) and an average rake of 165°. The secondary slip asperity of 12×12 km in size, with a local peak slip of 2.64 m at a depth of ~15 km, is found in the northern segment of the fault at 53.12 °N, 142.95 °E. This asperity is mainly characterized by the southwestwards thrust slip (maximum of 2.64 m) with a rake of ~50–60°.

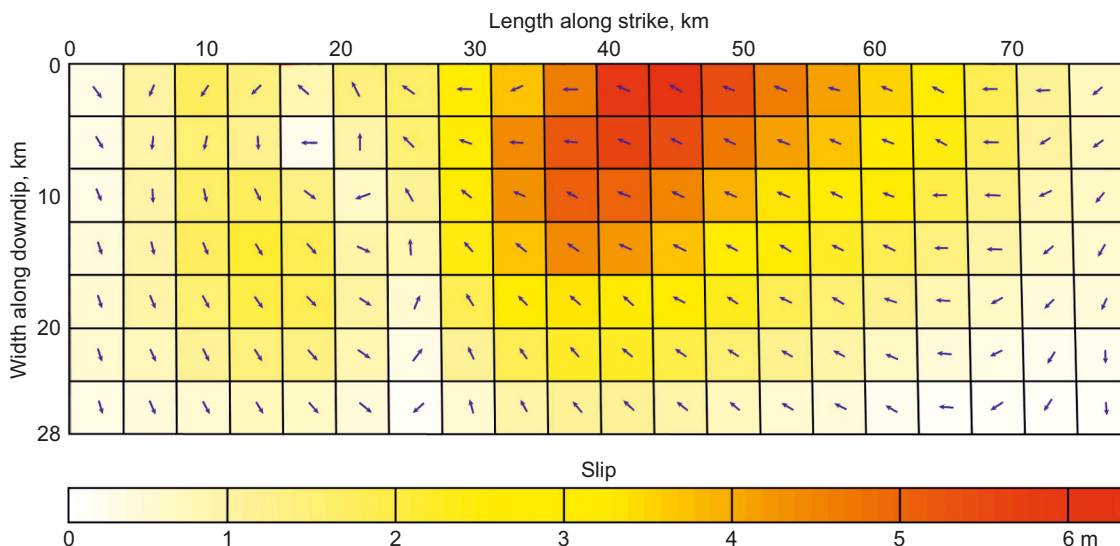


Fig. 4. The slip distribution of the Neftegorsk earthquake model. The slips in meters are shown by color below the model. The slip directions are indicated by blue arrows.

Рис. 4. Распределение смещений в модели очага Нефтегорского землетрясения. Смещение в метрах показано цветом под моделью. Направление смещений обозначено синими стрелками.

The average model slip rake is 165.7°. The average model slip on the fault plane is approximately 1.91 m. An earthquake stress drop estimate, D_r , was 11.3 MPa. Assuming a shear modulus of 30 GPa, the model has a total moment of 7.49×10^{19} N·m equal to a moment magnitude of 7.2, slightly larger than the [USGS..., 2022] and [Global CMT..., 2022] solutions.

4. DISCUSSION

The Neftegorsk earthquake was the first recorded seismic event with $M \sim 7.0$ that occurred at the northern part of junction between the Eurasian and the North American (Okhotsk) plates. The earthquake had a strike-slip faulting focal mechanism, which did not agree with the recent regional geodynamic situation, and differed from the earlier $M > 7.0$ events which had thrust faulting mechanisms and occurred at the boundary of the lithospheric plates (see Fig. 1, inset).

The results of teleseismic body wave inversion allowed estimating the rupture process and suggesting that the earthquake included several subevents. [Katsumata et al., 2004; Polets, Zlobin, 2017] concluded that the Neftegorsk earthquake corresponded to two subevents having almost the same mechanism. [Arefiev et al., 2000] concluded that the earthquake consisted of four subevents, with the northern one had a reverse slip distribution differing from the others. Our geodetic slip model suggests two asperities with different slip distributions. Larger slip asperity is characterized by the right-lateral strike-slip motion corresponding to the earthquake focal mechanism, whereas the northern asperity has reverse fault mechanism. The geodetic moment of our slip model is similar to other geodetic solutions, though it is considerably larger (~50%), than the seismic moment of the earthquake point source. The GPS and InSAR data obtained 2 months and 2 weeks after the

event, respectively, may include postseismic deformations and thus resulting in some overestimation. On the other hand, our results are close to the seismic moment derived by finite fault modeling based on the teleseismic waveform data. It is possible that [Polets, Zlobin, 2017] developed the finite fault model with a longer (~23 s) energy release than was estimated by the point source models.

The slip models from geodetic and teleseismic inversions are generally consistent with each other (Table 1). The main discrepancy lies in geometric parameters of the source (fault length and width) and average slip. To compare the models, we calculated the coseismic displacements at near-field GPS points. The teleseismic slip model differs from the geodetic results. It has a worse agreement with the measured coseismic displacements. RMSE for the teleseismic slip model is 0.89 whereas in the geodetic models it does not exceed the value of 0.58. We found that the observed near-field coseismic displacements, especially at some stations close to the surface rupture, do not fit well with the slip model [Polets, Zlobin, 2017] in terms of both amplitude and direction. This incongruity primarily relates to the location of the model earthquake source, with the epicenter (latitude = 52.629°; longitude = 142.827°) about 4 km south of the surface fault [USGS..., 2022].

There are also some differences in the patterns of the slip distributions, although both seismological and geodetic models show close values of the maximum slip in two areas of finite fault model: ~6.5 m and ~2.5 m. The discrepancy lies in the location of the peak slip, which occurs at a much shallower depth in our model (~2 km) than in the model of [Polets, Zlobin, 2017] (~14 km). Joint inversions of the geodetic and teleseismic waveform data for other large earthquakes show that the slip depth is usually constrained better by the geodetic data, at least for depths shallower than 20 km [Pritchard, Fielding, 2008].

The estimated surface coseismic slip agrees well with the measured displacements in the surface rupture [Shimamoto et al., 1996] (Fig. 5). However, there are certain differences of the slip distributions. The maximum observed value of surface slip (8.1 m) is larger than the modeled value (6.36 m) and unusually large for an event of such magnitude [Arefiev et al., 2000]. Besides, the fragments of the

surface rupture may include significant non-linear local effects, which could cause these differences.

According to the seismic stress trigger theory, the occurrence of earthquake event will lead to stress redistribution at the epicenter and its surroundings. The stress change field is not only correlates highly with the aftershock distribution but also affects seismic risk of the surrounding

Table 1. Source parameters of the Neftegorsk earthquake from different data sources
Таблица 1. Параметры очага Нефтегорского землетрясения по различным данным

Source	United States Geological Survey [USGS..., 2022]	Global Centroid Moment Tensor [Global CMT..., 2022]	[Polets, Zlobin, 2017]	[Katsumata et al., 2004]	[Arefiev et al., 2000]	[Takahashi et al., 1995]	[Tobita et al., 1998]*	This study
Dataset	Teleseismic			Teleseismic, aftershock		GPS	InSAR	GPS
Latitude (N°)	52.629	53.03	52.629	52.64	-	-	-	52.87
Longitude (E°)	142.827	142.65	142.827	142.83	-	-	-	142.91
Strike (°)	107/197	287/196	196	196	196	197	194	200-194
Dip (°)	88/89	79/82	82	79	71	78	84	79
Rake (°)	-1/-178	8/169	171.8	-174	188	165	-	166
Focal depth (km)	11.5	23.6	11	9	6.7	-	-	-
Fault length (km)	-	-	80	30-60	46	35	48.1	78
Fault width (km)	-	-	36	15	12	15	14.5	28
Average slip (m)	-	-	1.45	2.3	3.9	5.5	3.4	1.91
Maximum slip (m)	-	-	6.62	-	-	-	7.1	6.36
Dr (bars)	-	-	-	4-11	-	-	-	11.3
Mo×10 ¹⁹ (N·m)	3.728	4.32	7.7	4.2	4.24	8.66	7.11	7.49
Mw	6.98	7.0	7.2	7.0	6.9	7.2	-	7.2
RMSE (m)	-	-	0.89	-	-	0.58	0.56	0.45

Note. * - there are presented the calculated average strike and dip values.
 Примечание. * - приведены вычисленные средние значения простирания и падения.

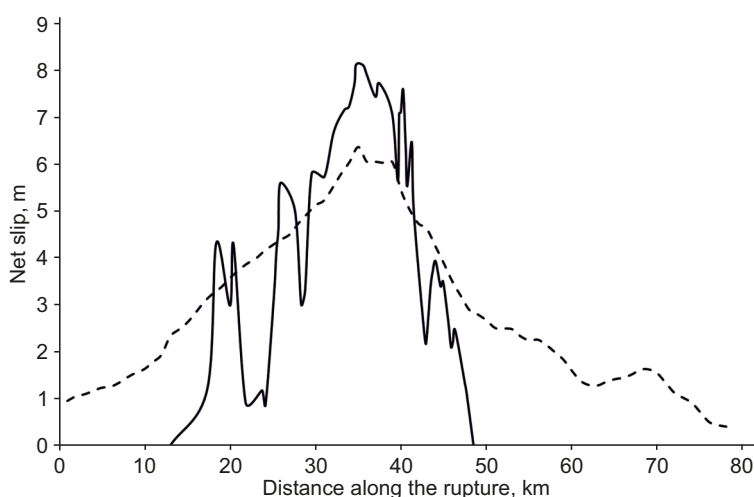


Fig. 5. Comparison between the modeled and measured displacements [Shimamoto et al., 1996] along surface rupture. The black solid line is the surface rupture displacements and the black dashed line is the modeled fault displacements. Distance along the rupture from its southern end.

Рис. 5. Сравнение модельных и измеренных смещений [Shimamoto et al., 1996] вдоль сейсморазрыва. Черная сплошная линия – измеренные, черная пунктирная – модельные смещения. Расстояние вдоль сейсморазрыва от его южного конца.

faults [Tabrez et al., 2008]. Based on the failure criterion, Coulomb stress changes are defined as follows:

$$\Delta CFS = \Delta\tau + \mu\Delta\sigma,$$

where $\Delta\tau$ is the change in shear stress on the fault plane (positive when sheared in the direction of fault slip); $\Delta\sigma$ is the change in normal stress (the tension direction of the fault is positive); and μ is the effective friction coefficient on the fault plane (the value involved here is equal to of 0.4, which was commonly used for Earth crust faulting [King et al., 1994]). We used the Coulomb 3.4 software package [Toda et al., 2011] to calculate the coseismic Coulomb stress changes resulting from the Neftegorsk earthquake.

The western part of the aftershock area bounded by the surface rupture includes more epicenters than the eastern part. The focal mechanism solutions of a large number of aftershocks are not clear. There were only determined five focal mechanisms of the aftershocks with a magnitude

$M=5.0-5.6$, corresponding to a thrust fault or thrust fault with an insignificant lateral component and different from the mainshock [USGS..., 2022]. The Coulomb stress changes of the optimal rupture plane can effectively explain the pattern of aftershock distributions [Shan et al., 2011, 2017]. Our results show that the coseismic Coulomb stress distribution resulting from the earthquake at an 11 km depth (depth of the mainshock from [USGS..., 2022]) is in good agreement with the aftershock distribution (Fig. 6).

The coseismic effect of the Neftegorsk earthquake caused a significant (more than 10 MPa) increase in stresses in the central segments of the Gyrgylaninsky and Hokkaido-Sakhalin faults and a decrease in stress in the northern part of the Gyrgylaninsky fault and in the Western Baikal fault. Most of the aftershocks are located in the areas where the Coulomb stress increased. So, the earthquake with a magnitude of 5.8 occurred in 2010 near the Gyrgylaninsky fault, where the Coulomb stress increased to 1 MPa (Fig. 7).

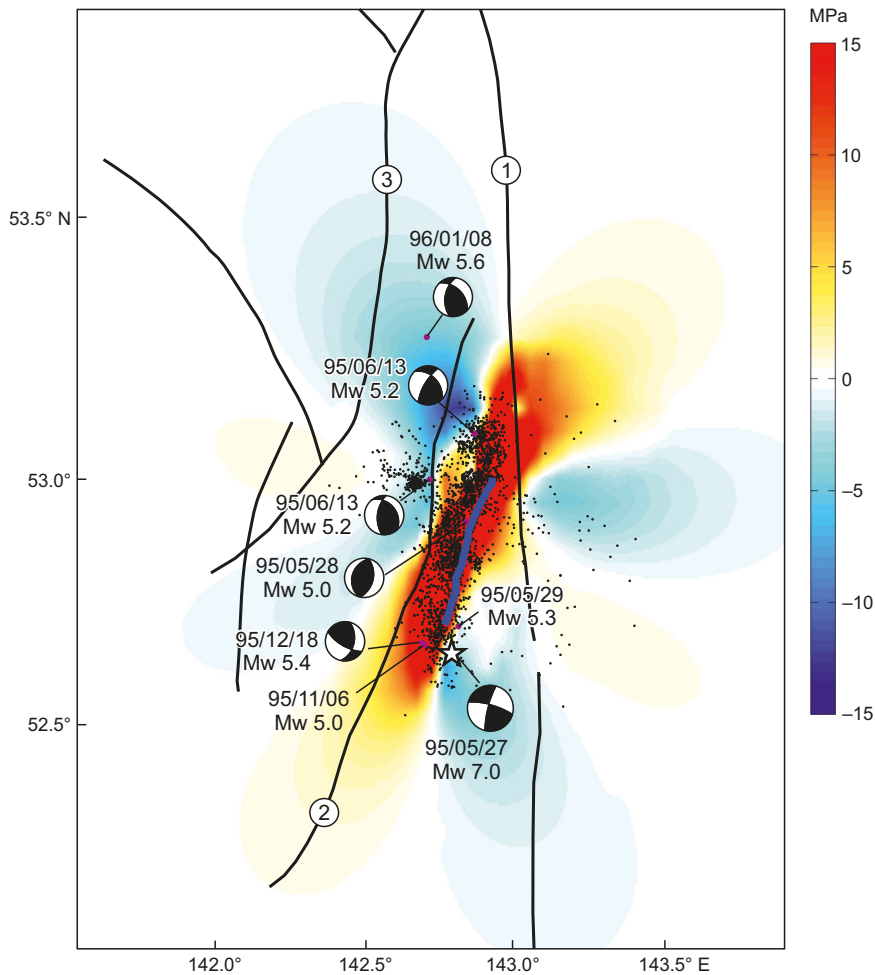


Fig. 6. Coseismic Coulomb stress changes from the Neftegorsk earthquake at a depth of 11 km. The focal mechanisms (lower hemisphere) and aftershocks $M>5.0$ for the period from May 28, 1995 to December, 1997 are shown after [USGS..., 2022]. Black dots are aftershocks from June 10 to July 8, 1995 [Arefiev et al., 2000; Katsumata et al., 2004]. Asterisk is the epicenter of the Neftegorsk mainshock. Faults are the same as in Fig. 1.

Рис. 6. Изменения кулоновских напряжений в результате Нefтегорского землетрясения на глубине 11 км. Механизмы очагов (в проекции нижней полусферы) и aftershockи с магнитудой $M>5.0$ за период с 28 мая 1995 г. по декабрь 1997 г. приведены по данным [USGS..., 2022]. Черные точки – aftershockи с 10 июня по 8 июля 1995 г. [Arefiev et al., 2000; Katsumata et al., 2004]. Звездочкой показан эпицентр Нefтегорского землетрясения. Разломы аналогичны рис. 1.

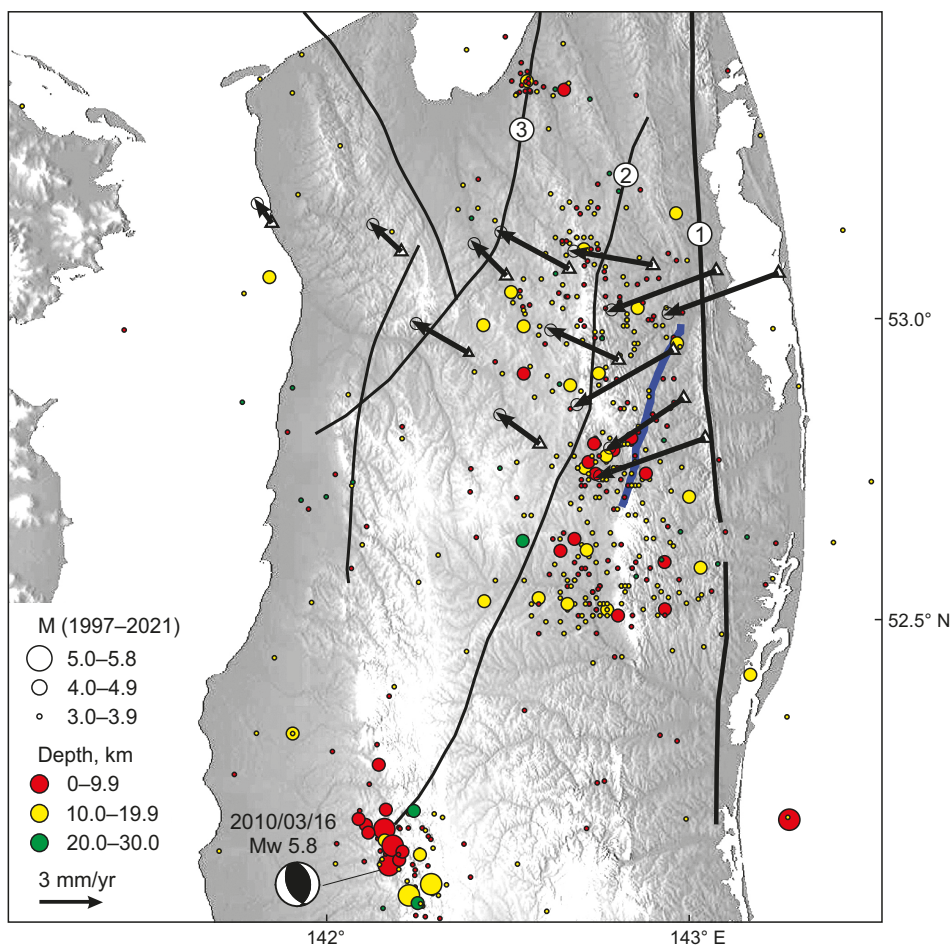


Fig. 7. Interseismic GPS velocities of the North Sakhalin relative to the stable Eurasian Plate for the period 2003–2013. The velocity error ellipses correspond to 95 % confidence interval. The circles are earthquake epicenters for the period 1997–2021 from [GS RAS..., 2022]. The focal mechanism of the 2010 Mw=5.8 earthquake is shown after [USGS..., 2022]. Faults are the same as in Fig. 1.

Рис. 7. Межсейсмические скорости GPS-пунктов северной части о. Сахалин относительно Евразийской плиты за период 2003–2013 гг. Эллипсы ошибок скоростей соответствуют 95 %-ному доверительному интервалу. Показаны эпицентры землетрясений за период 1997–2021 гг. по данным [GS RAS..., 2022]. Механизм очага землетрясения 2010 г. Mw=5.8 приведен по данным [USGS..., 2022]. Разломы аналогичны рис. 1.

This is the strongest event ever occurred in this area since 1906.

Trenching of the Hokkaido – Sakhalin fault as well as radiocarbon dating of the faulted strata and landscape features showed that fault-related strong earthquakes took place with intervals from several hundred to one or two thousand years [Kozhurin, 2004]. The seismic risk in this area increases due to the stress increase caused by the Neftegorsk earthquake. Although recent seismicity of this fault is weak, it is able to accumulate the strain energy sufficient for M=7.0–7.5 earthquakes.

Geodynamic GPS observations at points in the northern part of Sakhalin Island, started in 2003, have revealed the character of deformation of the earth surface after the Neftegorsk earthquake [Prytkov, Vasilenko, 2018]. The latitudinal components of the interseismic velocities gradually increase from the west (0.6 mm/year) to the east (3.7 mm/year) relative to the Eurasian Plate (Fig. 7). To

the east of the Neftegorsk surface rupture, the velocities change their sublatitudinal directions to the southwestern ones while the displacement rate reaches 5.4 mm/year (the average uncertainty 1 σ is 1.1 mm). The strain accumulations in the surroundings of the surface rupture with rates of ~4 mm/year implies that a recurrence time for an event like the Neftegorsk earthquake may be very long, at least a thousand years, though this is very uncertain due to the short GPS observation period. As compared with our results, trenching of the surface rupture [Rogozhin, 1995] yielded a shorter, about 400-year long recurrence interval between strong fault-related earthquakes.

5. CONCLUSION

The geodetic data was used to invert the source parameters and fault slip distribution of the May 28, 1995 earthquake in North Sakhalin. Based on the aftershock distribution and field investigations, we identified the fault trace,

which strikes 200° in the northern part and 196° in the southern part. We determined the source parameters using the optimization procedure, which was realized by the steepest descent method incorporating the layered crust structure.

The inversion denotes that a significant slip area extends to 78 km along the strike and dips down at 28 km. Our model suggests two asperities with different slip distributions. Larger slip asperity is characterized by the right-lateral strike-slip motions with a maximum slip of 6.36 m near the surface and corresponds to the earthquake focal mechanism, whereas northern asperity has a reverse fault mechanism with a local peak of 2.64 m at a depth of 15 km.

The value of estimated geodetic moment released by the slip model of Neftegorsk earthquake is 7.49×10^{19} N·m and equivalent to an event of $M_w=7.2$. The Coulomb stress distribution resulting from the earthquake is in a good agreement with the aftershock distribution, most of which occurred in the area where the stress was increased. A large slip value and the absence of strong aftershocks could indicate that the strain, accumulated over a long time, was almost totally released during the mainshock. In the near future, according to the Coulomb stress change, more attention should be paid to the potential strong earthquakes at the surrounding faults. The recent GPS velocities in the surface rupture surroundings mean that the recurrence time for an event like the Neftegorsk earthquake may be more than a thousand years.

6. CONTRIBUTION OF THE AUTHORS / ЗАЯВЛЕННЫЙ ВКЛАД АВТОРОВ

Both authors made an equivalent contribution to this article, read and approved the final manuscript.

Авторы внесли эквивалентный вклад в подготовку рукописи, прочли и одобрили финальную версию перед публикацией.

7. DISCLOSURE / РАСКРЫТИЕ ИНФОРМАЦИИ

Both authors declare that they have no conflicts of interest relevant to this manuscript.

Авторы заявляют об отсутствии конфликта интересов, связанного с этой рукописью.

8. REFERENCES / ЛИТЕРАТУРА

Arefiev S., Rogozhin E., Tatevossian R., Rivera L., Cisternas A., 2000. The Neftegorsk (Sakhalin Island) 1995 Earthquake: a Rare Interplate Event. *Geophysical Journal International* 143 (3), 595–607. <https://doi.org/10.1046/j.1365-246X.2000.00234.x>.

DeMets C., Gordon R.G., Argus D.F., 2010. Geologically Current Plate Motions. *Geophysical Journal International* 181 (1), 1–80. <https://doi.org/10.1111/j.1365-246X.2009.04491.x>.

Global CMT Catalog, 2022. Available from: <https://www.globalcmt.org/CMTsearch.html> (Last Accessed May 4, 2022).

GS RAS Seismic Catalogues and Bulletin, 2022. Available from: <http://www.ceme.gsras.ru/new/eng/catalog/> (Last Accessed May 4, 2022).

Katsumata K., Kasahara M., Ichiyangi M., Kikuchi M., Sen R., Kim C.U., Ivaschenko A., Tatevossian R., 2004. The 27 May 1995 Ms 7.6 Northern Sakhalin Earthquake: An Earthquake on an Uncertain Plate Boundary. *Bulletin of the Seismological Society of America* 94 (1), 117–130. <http://doi.org/10.1785/0120020175>.

Kharakhinov V.V., 2010. Oil-Gas Geology of the Sakhalin Region. Nauchnyy Mir, Moscow, 276 p. (in Russian). [Харахинов В.В. Нефтегазовая геология Сахалинского региона. М.: Научный мир, 2010. 276 с.].

King G.C.P., Stein R.S., Lin J., 1994. Static Stress Changes and the Triggering of Earthquakes. *Bulletin of the Seismological Society of America* 84 (3), 935–953. DOI:10.1785/BSSA0840030935.

Kozhurin A.I., 2004. Active Faulting at the Eurasian, North American and Pacific Plates Junction. *Tectonophysics* 380 (3–4), 273–285. <https://doi.org/10.1016/j.tecto.2003.09.024>.

Okada Y., 1985. Surface Deformation Due to Shear and Tensile Faults in a Halfspace. *Bulletin of the Seismological Society of America* 75 (4), 1135–1154. <https://doi.org/10.1785/BSSA0750041135>.

Polets A.Yu., Zlobin T.K., 2017. 1995 Neftegorsk Earthquake Source Inversion Model. *Vestnik of the Far East Branch of the Russian Academy of Science* 191 (1), 38–42 (in Russian) [Полец А.Ю., Злобин Т.К. Моделирование очага методом инверсии волновых форм на примере Нefтегорского землетрясения 1995 года // Вестник ДВО РАН. 2017. Т. 191. № 1. С. 38–42].

Pritchard M.E., Fielding E.J., 2008. A Study of the 2006 and 2007 Earthquake Sequence of Pisco, Peru, with InSAR and Teleseismic Data. *Geophysical Research Letters* 35 (9), L09308. <https://doi.org/10.1029/2008GL033374>.

Prytkov A.S., Vasilenko N.F., 2018. Earth Surface Deformation of the Sakhalin Island from GPS Data. *Geodynamics & Tectonophysics* 9 (2), 503–514 (in Russian) [Прытков А.С., Василенко Н.Ф. Деформации земной поверхности острова Сахалин по данным GPS-наблюдений // Геодинамика и тектонофизика. 2018. Т. 9. № 2. С. 503–514]. <https://doi.org/10.5800/GT-2018-9-2-0358>.

Rogozhin E.A., 1995. The Neftegorsk Earthquake May 27 (28), 1995: Geological Evidence and Tectonic Setting. In: *The Neftegorsk Earthquake May 27 (28), 1995. Information Analysis Bulletin of the Federal System of Seismological Observations and Earthquake Prediction. Spec. Iss. Moscow*, p. 80–94 (in Russian) [Рогожин Е.А. Нефтегорское землетрясение 27 (28) мая 1995 г.: геологические проявления и тектоническая позиция очага // Нефтегорское землетрясение 27(28).05.1995 г.: Информационно-аналитический бюллетень ФССН. Спец. выпуск. М., 1995. С. 80–94].

Segall P., Harris R., 1987. Earthquake Deformation Cycle on the San Andreas Fault near Parkfield, California. *Journal of Geophysical Research* 92 (B10), 10511–10525. <https://doi.org/10.1029/JB092iB10p10511>.

Shan B., Xiong X., Zheng Y., Wei S., Wen Y., Jin B., Ge C., 2011. The Co-Seismic Coulomb Stress Change and Expected Seismicity Rate Caused by 14 April 2010 Ms=7.1 Yushu, China, Earthquake. *Tectonophysics* 510 (3–4), 345–353. <https://doi.org/10.1016/j.tecto.2011.08.003>.

Shan B., Zheng Y., Liu C.L., Xie Z.J., Kong J., 2017. Coseismic Coulomb Failure Stress Changes Caused by the 2017 M7.0 Jiuzhaigou Earthquake, and Its Relationship with the 2008 Wenchuan Earthquake. *Science China Earth Sciences* 60, 2181–2189. <https://doi.org/10.1007/s11430-017-9125-2>.

Shimamoto T., Watanabe M., Suzuki Y., 1995. Surface Faults and Damage Associated with the 1995 Neftegorsk Earthquake. In: *The May 27(28), 1995 Neftegorsk Earthquake. Information Analysis Bulletin of the Federal System of Seismological Observations and Earthquake Prediction. Spec. Iss. Moscow*, p. 101–116 (in Russian) [Шимамото Т., Ватанабе М., Судзуки Я. Поверхностные разрывы, связанные с Нефтегорским землетрясением 27(28) мая 1995 г. // Нефтегорское землетрясение 27(28).05.1995 г.: Информационно-аналитический бюллетень ФССН. Спец. выпуск. М., 1995. С. 101–116].

Shimamoto T., Watanabe M., Suzuki Y., Kozhurin A., Strel'tsov M., Rogozhin E., 1996. Surface Faults and Damage Associated with the 1995 Neftegorsk Earthquake. *The Journal of the Geological Society of Japan* 102 (10), 894–907.

Tabrez A.S., Freed A.M., Calais E., Manaker D.M., McCann W.R., 2008. Coulomb Stress Evolution in Northeastern Caribbean over the Past 250 Years due to Coseismic, Postseismic and Interseismic Deformation. *Geophysical Journal International* 174 (3), 904–918. <https://doi.org/10.1111/j.1365-246X.2008.03634.x>.

Takahashi H., Kasahara M., Vasilenko N., Kim C.U., Ivashchenko A., Kimata F., Seno T., 1996. Coseismic Deformation around the Northern Part of Epicentral Area of the 1995 North Sakhalin Earthquake Deduced from Geodetic Observations. In: *Report on North Sakhalin Earthquake and Its Disaster*. P. 191–202.

Takahashi H., Vasilenko N., Kimata F., Kasahara M., Seno T., Kim C.U., Ivashchenko A., 1995. Coseismic Deformation around the Northern Part of Epicentral Area of the 1995 North Sakhalin Earthquake Deduced from Geodetic Observations. In: *The May 27(28), 1995 Neftegorsk Earthquake.*

Information Analysis Bulletin of the Federal System of Seismological Observations and Earthquake Prediction. Spec. Iss. Moscow, p. 123–128 (in Russian) [Такахаси Х., Василенко Н., Кимата Ф., Касахара М., Сено Т., Ким Ч.У., Иващенко А. Косейсмические деформации в северной части эпицентральной зоны Нефтегорского землетрясения 1995 г. по данным геодезических наблюдений // Нефтегорское землетрясение 27(28).05.1995 г.: Информационно-аналитический бюллетень ФССН. Спец. выпуск. М., 1995. С. 123–128].

Tobita M., Fujiwara S., Ozawa S., Rosen P.A., Fielding E.J., Werner C.L., Murakami M., Nakagawa H. et al., 1998. Deformation of the 1995 North Sakhalin Earthquake Detected by JERS-1/SAR Interferometry. *Earth Planets Space* 50, 313–325. <https://doi.org/10.1186/BF03352118>.

Toda S., Stein R.S., Sevilgen V., Lin J., 2011. Coulomb 3.3. Graphic-Rich Deformation and Stress-Change Software for Earthquake, Tectonic, and Volcano Research and Teaching. User Guide. USGS Open-File Report 2011–1060, 63 p.

USGS Earthquake Hazards Program, 2022. Available from: <https://earthquake.usgs.gov/earthquakes/search/> (Last Accessed May 4, 2022).

Vasilenko N.F., Prytkov A.S., Kasahara M., Takahashi H., 2015. Recent Geodynamics of the Northern Sakhalin before and after May 27 (28), 1995 Mw 7.0 Neftegorsk Earthquake. In: *Geodynamical Processes and Natural Hazards. Lesson of Neftegorsk: Proceedings of the All-Russian Scientific Conference with International Participation (May 26–30, 2015, Yuzhno-Sakhalinsk)*. Vol. 1. Dal'nauka, Vladivostok, p. 13–16 (in Russian) [Василенко Н.Ф., Прытков А.С., Касахара М., Такахаси Х. Современная геодинамика Северного Сахалина до и после Нефтегорского землетрясения 27 (28) мая 1995 г. Mw=7.0 // Геодинамические процессы и природные катастрофы. Опыт Нефтегорска: Сборник трудов Всероссийской научной конференции с международным участием (26–30 мая 2015 г., Южно-Сахалинск). Владивосток: Дальнаука, 2015. Т. 1. С. 13–16].

Wang R., Diao F., Hoechner A., 2013. SDM – A Geodetic Inversion Code Incorporating with Layered Crust Structure and Curved Fault Geometry. *General Assembly European Geosciences Union, Geophysical Research Abstracts* 15, EGU2013-2411-1.